Supplementary information

Utilizing non-stoichiometry in $Nd_2Zr_2O_7$ pyrochlore: Exploring superior ionic conductors

P. Anithakumari[1], V. Grover[1]*, C. Nandi[2], K. Bhattacharyya[1] and A. K. Tyagi[1]

[1]*Chemistry Division, Bhabha Atomic Research Centre, Mumbai- 400085, India*

[2]*Radio Metallurgy Division, Bhabha Atomic Research Centre, Mumbai- 400085, India*

Fig. 1 The Nd 4p XPS spectra recorded for the nominal compositions $Nd_{1.6}Zr_{2.4}O_{7.2}$ and $Nd_{1.8}Zr_{2.2}O_{7.1}$
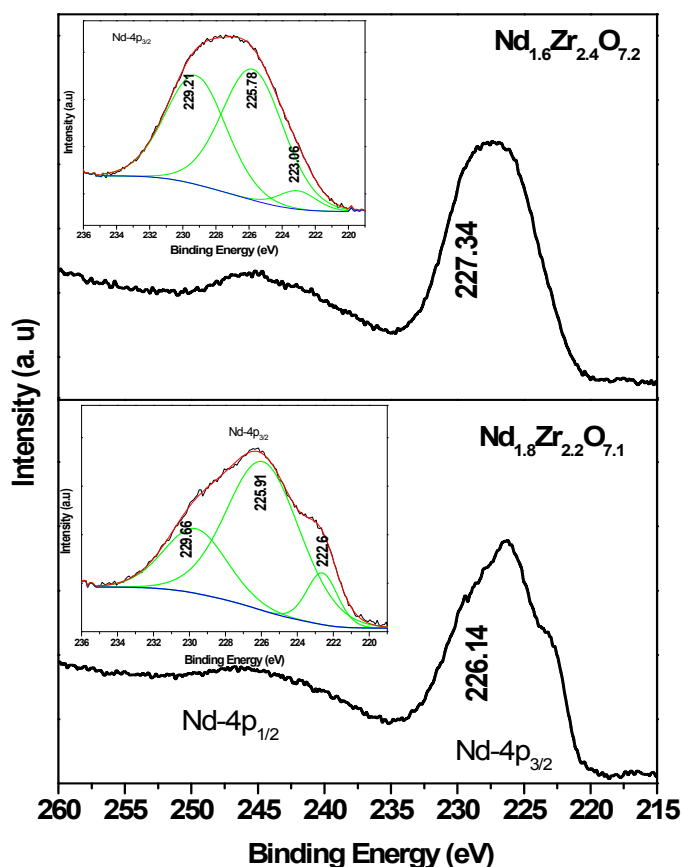
Table 1: The data obtained after deconvolution of Nd $4p_{3/2}$ peak for the two nominal compositions $Nd_{1.6}Zr_{2.4}O_{7.2}$ and $Nd_{1.8}Zr_{2.2}O_{7.1}$

Peak	223.06	225.78	229.21	$Nd_{1.6}Zr_{2.4}O_{7.2}$
FWHM	2.67	4.39	4.29	
Area	17002	198150	161043	
Area(%)	4.52	52.66	42.83	
Peak	222.61	225.91	229.66	$Nd_{1.8}Zr_{2.2}O_{7.2}$
FWHM	2.02	4.79	4.11	
Area	34998	239551	89161	
Area(%)	9.62	65.86	24.53	

Fig. 2. The Zr 3p XPS spectra recorded for the nominal compositions $Nd_{1.6}Zr_{2.4}O_{7.2}$ and $Nd_{1.8}Zr_{2.2}O_{7.1}$
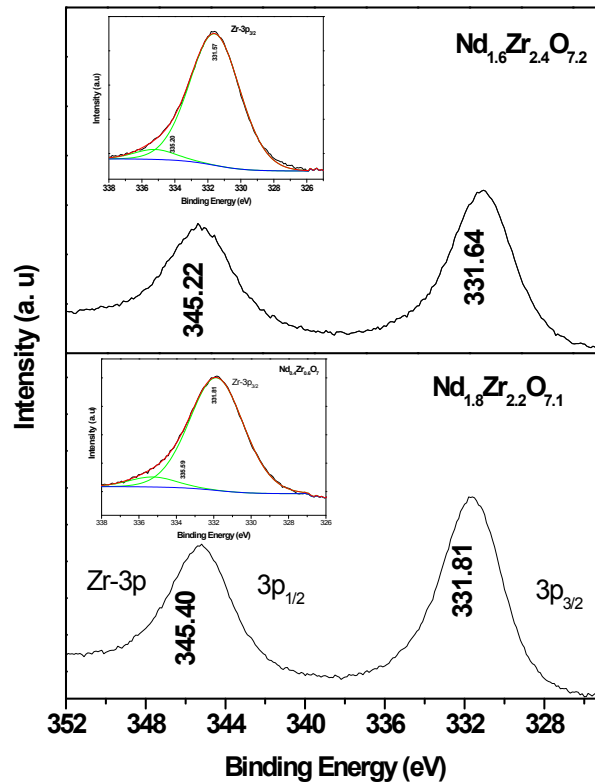
Table 2: The data obtained after deconvolution of Zr 3p$_{3/2}$ peak for the two nominal compositions Nd$_{1.6}$Zr$_{2.4}$O$_{7.2}$ and Nd$_{1.8}$Zr$_{2.2}$O$_{7.1}$

Peak	331.56	334.48	**Nd$_{1.6}$Zr$_{2.4}$O$_{7.2}$**
FWHM	3.44	2.64	
Area	649812	37448	
Area(%)	94.55	5.45	
Peak	331.85	335.25	**Nd$_{1.8}$Zr$_{2.2}$O$_{7.2}$**
FWHM	3.45	2.87	
Area	439713	340645	
Area(%)	92.81	7.19	

Fig. 1 represents XPS spectrum of the Nd 4p$_{1/2}$ and 4p$_{3/2}$ and the inset shows the respective deconvoluted spectrum of the Nd 4p$_{3/2}$ peak for the two nominal compositions Nd$_{1.6}$Zr$_{2.4}$O$_{7.2}$ and Nd$_{1.8}$Zr$_{2.2}$O$_{7.1}$. Three peaks at 223.1, 225.8 and 229.2 eV could be obtained upon deconvolution of Nd 4p$_{3/2}$ peaks. The quantitative data associated with these peaks determined using the CASA software is also presented in the **Table 1**. These being Nd^{3+}-deficient compositions, three types of environments for Nd^{3+} are expected. Vacant A (Nd^{3+}) -sites, normal Nd^{3+} pyrochlore sites and Nd^{3+} in vicinity of Zr^{4+}. Due to higher electron density at Nd^{3+} in vicinity of vacancy, the least binding energy would represent the Nd^{3+}- vacancy states. The other two would be Nd^{3+} in A-site in pyrochlore lattice and the other where in the lattice sites Nd^{3+} are replaced by the Zr^{4+}. The Nd^{3+} ions in the vicinity of Zr^{4+} will experience lesser electron density and hence should possess higher binding energy. Thus, the component at 229.2 eV represents Nd^{3+} in Zr^{4+} vicinity and the component at 225.8 eV should correspond to the Nd in the usual A-site in pyrochlores. The great prevalence of disorder would imply greater fraction of the component at 229.2 eV. It is obvious from Fig. 1 that the nominal composition Nd$_{1.6}$Zr$_{2.4}$O$_{7.2}$ possess greater fraction of Nd^{3+} in vicinity of Zr^{4+} in similar environment implying it has higher disorder. Further, if the extent of order has to increase from Nd$_{1.6}$Zr$_{2.4}$O$_{7.2}$ to Nd$_{1.8}$Zr$_{2.2}$O$_{7.1}$, there should be an increase in average co-ordination number of Nd^{3+} which should manifest in lower average binding energy. As is obvious from the figure that average binding energy decreases on proceeding from the nominal composition Nd$_{1.6}$Zr$_{2.4}$O$_{7.2}$ to Nd$_{1.8}$Zr$_{2.2}$O$_{7.1}$ thus supporting greater order in latter.

Similarly, **Fig. 2** depicts Zr -3p XPS peaks and the inset shows the deconvoluted 3-$p_{3/2}$ peak for the two nominal compositions. The respective data obtained after deconvolution and fitting are shown **Table 2**. We must state that not much is evident from the XPS data on Zr except that a slight increase in average B.E. indicates towards decrease in average co-ordination number of Zr on proceeding from $Nd_{1.6}Zr_{2.4}O_{7.2}$ to $Nd_{1.8}Zr_{2.2}O_{7.1}$. This is in accordance in increase in order of system. An increase in order would try to increase the amount of Zr in 6-fold co-ordination.